Electronic Supplementary Material (ESI) for CrystEngComm.

Electronic Supporting Information

Nanostructured zeolite with brain-coral morphology and tailored acidity: A self-organized hierarchical porous material with MFI topology

Esun Selvam,[a] Rajesh K. Parsapur,[b] Carlos E. Hernandez-Tamargo[b,c], Nora H. de Leeuw[c,d] and Parasuraman Selvam[b,e,f*]

---

[a]*Department of Chemical Engineering, National Institute of Technology-Trichy, Tiruchirappalli 620 015, Tamil Nadu, India. Present Address: Department of Chemical and Biomolecular Engineering, University of Delaware, Newark, DE 19716-3110, United States of America*

[b]*National Centre for Catalysis Research and Department of Chemistry, Indian Institute of Technology-Madras, Chennai 600 036, Tamil Nadu, India. E-Mail: selvam@iitm.ac.in*

[c]*School of Chemistry, Cardiff University, Cardiff CF10 3AT, United Kingdom*

[d]*School of Chemistry, University of Leeds, Leeds LS2 9JT, United Kingdom*

[e]*School of Chemical Engineering and Analytical Science, The University of Manchester, Manchester M13 9PL, United Kingdom*

[f]*Department of Chemical and Process Engineering, University of Surrey, Guildford, Surrey GU2 7XH, United Kingdom*

Reaction Scheme

A schematic representation of the influence of reaction conditions as well as the influence of different types of acid sites on the tertiary butylation of phenol is given below (Scheme 1).[1]

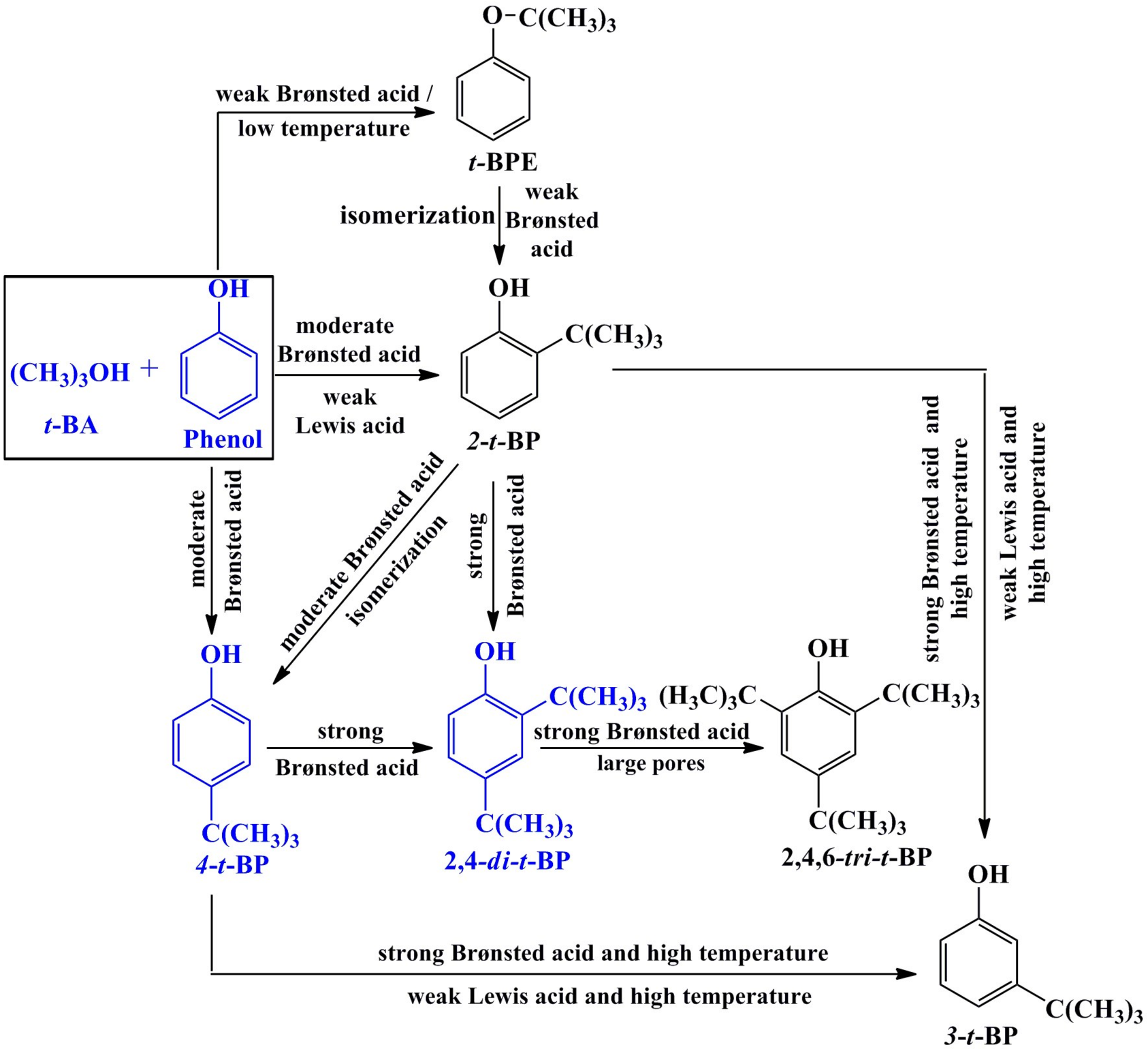

Scheme S1. Reaction pathways for the acid-mediated tertiary butylation of phenol reaction.

Synthesis and Characterization

The zeolites, *nano*-ZSM-5 (*n*-ZSM-5) and conventional or bulk ZSM-5 (*c*-ZSM-5), were hydrothermally synthesized by the standard templating strategy. Specifically, fabricated stainless-steel autoclaves (Grade SS-316) were used for the preparation these materials. To avoid contamination from the reaction vessel, cylindrical Teflon-containers enclosed autoclaves which can withstand high temperatures and pressure for a long time are routinely used for the synthesis (Figure S1). The as-synthesized materials of both nano-ZSM-5 and bulk-ZSM-5 were calcined in a temperature programmed tubular furnace (Figure S2) under flowing air, nitrogen and/or oxygen (40−60 *mL* min^{-1}) atmosphere by placing about 4 *g* of the sample in the center of the quartz reactor that is packed on both ends with ceramic wool. All the samples were systematically characterized by various analytical, spectroscopic, and microscopic techniques as described in the experimental section.

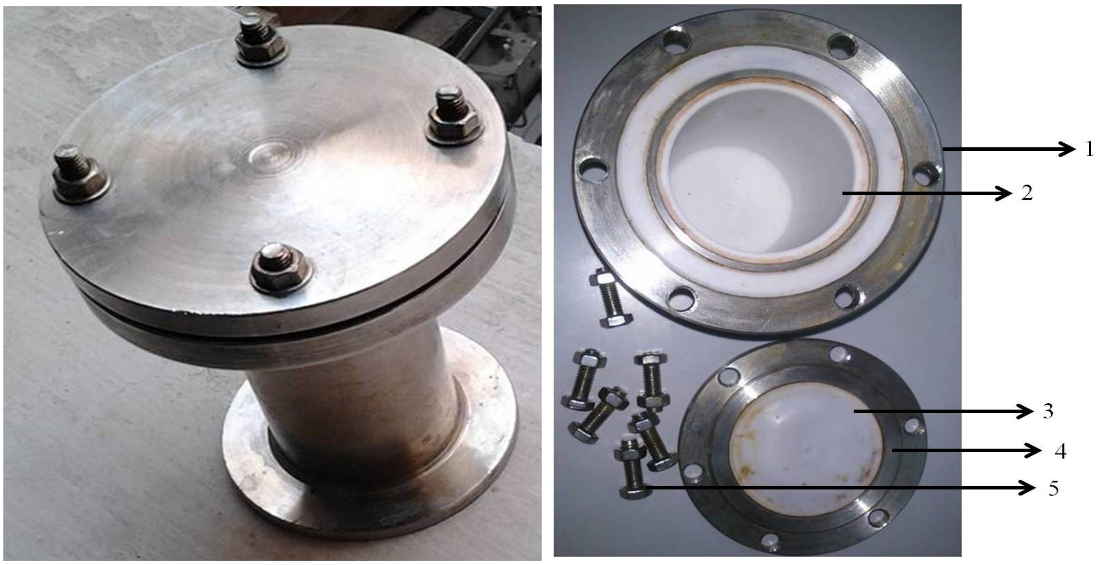

Figure S1. The reactor used for hydrothermal synthesis of zeolites: (1) Stainless steel jar; (2) Teflon container; (3) Teflon lid; (4) Stainless steel lid; (5) Stainless steel bolt.

Catalytic Activity Test

The tertiary butylation of phenol reaction[1] was carried out using the down-flow fixed-bed reactor (Figure S3). Prior to the reaction, the catalyst bed was activated and subsequently cooled to reaction temperature under nitrogen atmosphere. After stabilizing the temperature, the reactant mixture, *viz.,* phenol and *tertiary*-butyl alcohol (*t*-BA), with a desired ratio and weight hour space velocity (WHSV) was fed into the reactor using a liquid injection (reactant) pump (Miclins) and nitrogen as the carrier gas. The gaseous products were cooled, and the condensed liquid products were collected every 1 *h* period. The products were identified by gas chromatography.

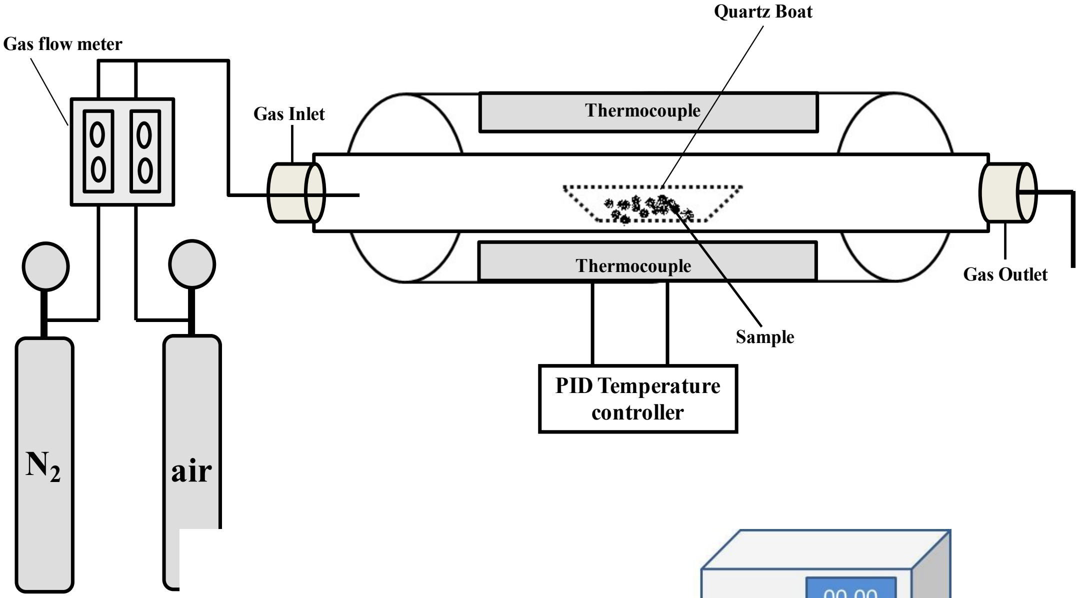

Figure S2. Schematic diagram of a tubular furnace set-up.

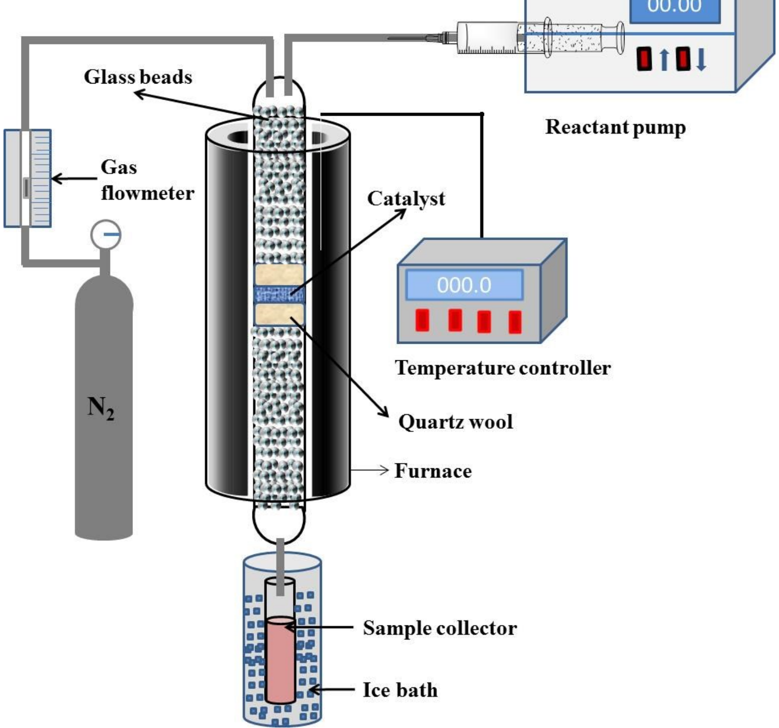

Figure S3. Schematic diagram of down-flow fixed-bed reactor.

Modelling Studies

We modelled the pure-silica and Al-substituted zeolite MFI under periodic boundary conditions (PBC) using the density functional theory (DFT) approximation as implemented in the plane wave code *Vienna Ab-Initio Simulation Package* (VASP).[2,3]

The definition proposed by Perdew, Burke, and Ernzerhof (PBE) for the general gradient approximation (GGA) was used to produce the valence Kohn-Sham orbitals of the system following a self-consistent procedure.[4,5]☐ A basis set of plane waves was used to treat explicitly the valence states whilst their nodal features and the core states were described by the projector-augmented-wave (PAW) method.[6,7]☐

Owing to the large dimension of the unit cell of zeolite MFI, only the Γ point was necessary during the numeric integration within the Brillouin zone.[8] The Gaussian smearing method accounted for the occupation of the electronic bands and the integration over the Γ point during the electronic relaxation, with widths of 0.05 eV for the zeolite and the NH_3+zeolite system, and 0.01 eV for the NH_3 molecule in the gas phase.[9–11]☐ We adopted convergence thresholds of 10^{-5} eV and 0.03 eV/Å for the electronic and structural optimizations, respectively.

We have also included Grimme's correction to the DFT energy to describe the dispersion interactions within the zeolite and between the zeolite and the NH_3 molecule, with a cut-off of 12 Å for the pairwise atomic interactions. The damping function of Becke-Johnson was selected to prevent near-singularities at small distances and the double counting of correlation effects at intermediate distances.[12,13]

The unit cell of zeolite MFI was used in all calculations concerning the adsorption of NH_3 at the internal and external surfaces. In the case of the external surface, a slab model was employed, saturating the dangling Si-O bonds with H atoms, thus forming silanol groups as shown in Figure S7. A vacuum layer of 18 Å was added at the top of the slab and along the normal direction to the external surface to reduce the interaction between periodic images.

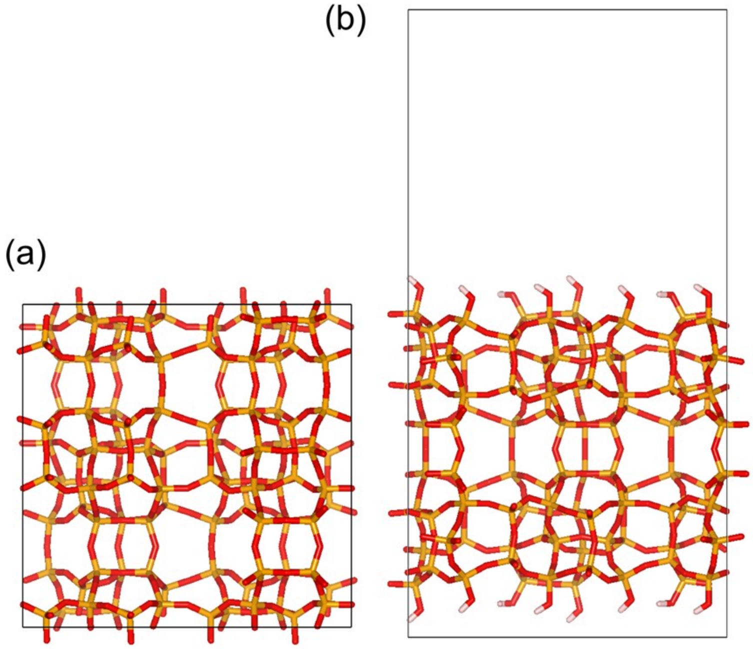

Figure S4: Representation of the structure of zeolite MFI used in the calculations. (a) Bulk, used for the adsorption of NH_3 at the internal surface. (b) Slab, used for the adsorption of NH_3 at the external surface. The black lines mark the limit of the box used under periodic boundary conditions. Color code: O (red), Si (orange).

Nano-zeolite Aggregation

The understanding of the nanoparticle aggregation is important for the rational design of reactors for high-throughput synthesis of nanoparticles with controlled properties. In this regard, the formation of self-assembled nano-zeolite structures are realized *via* nucleation and growth process. In general, at length scales < 1 *nm* nucleation resulting from high concentration of precursors takes place and nuclei grow rapidly into nanoparticles (10-20 *nm*).[14] In these length scales, Brownian motion leads to nanoparticle aggregation[15] resulting in aggregates of > 100 *nm* as shown below both by SEM and TEM images (Fig. S5 and S6).

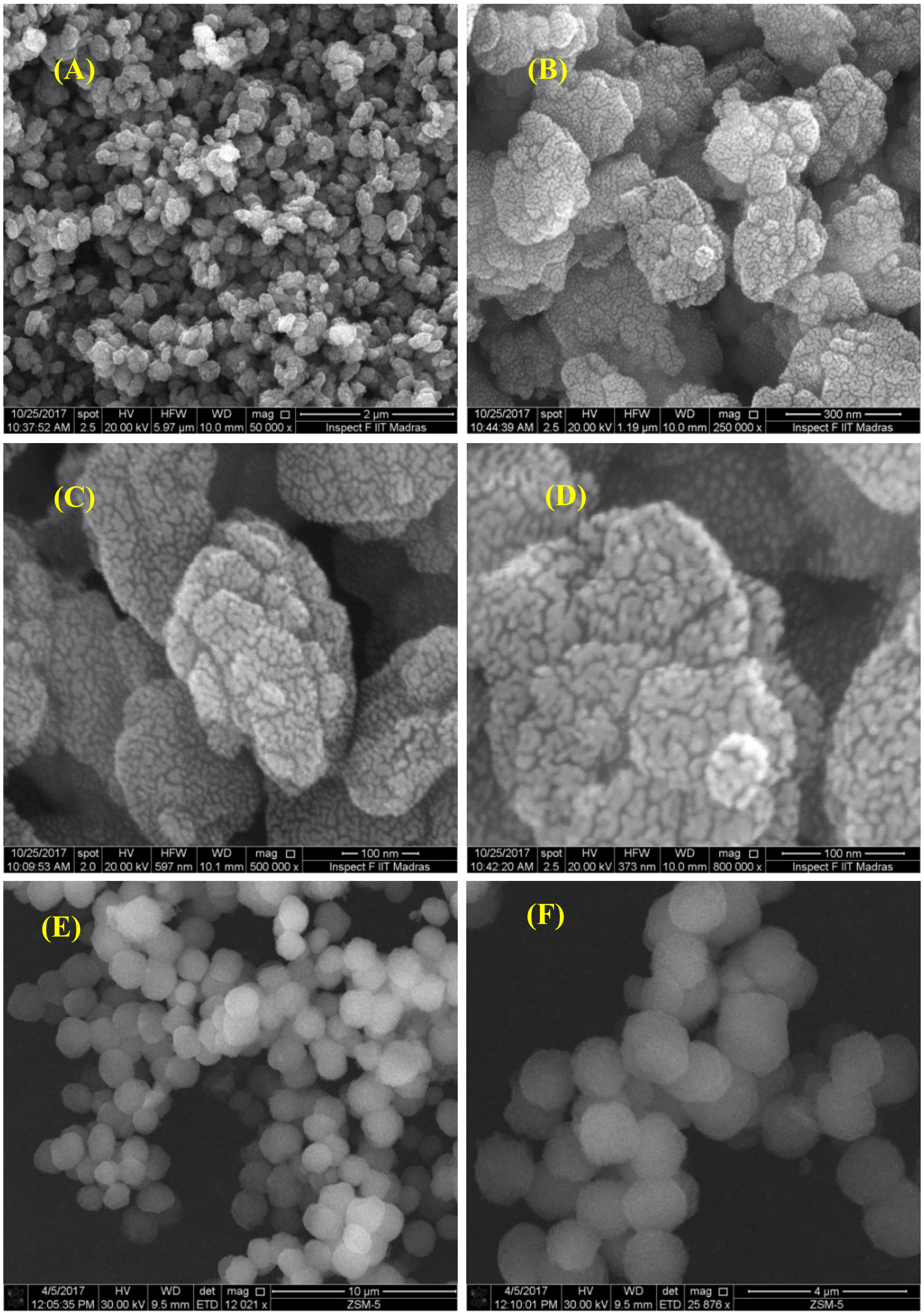

Figure S5. SEM images of *n*-ZSM-5 (A-D) and ZSM-5 (E,F).

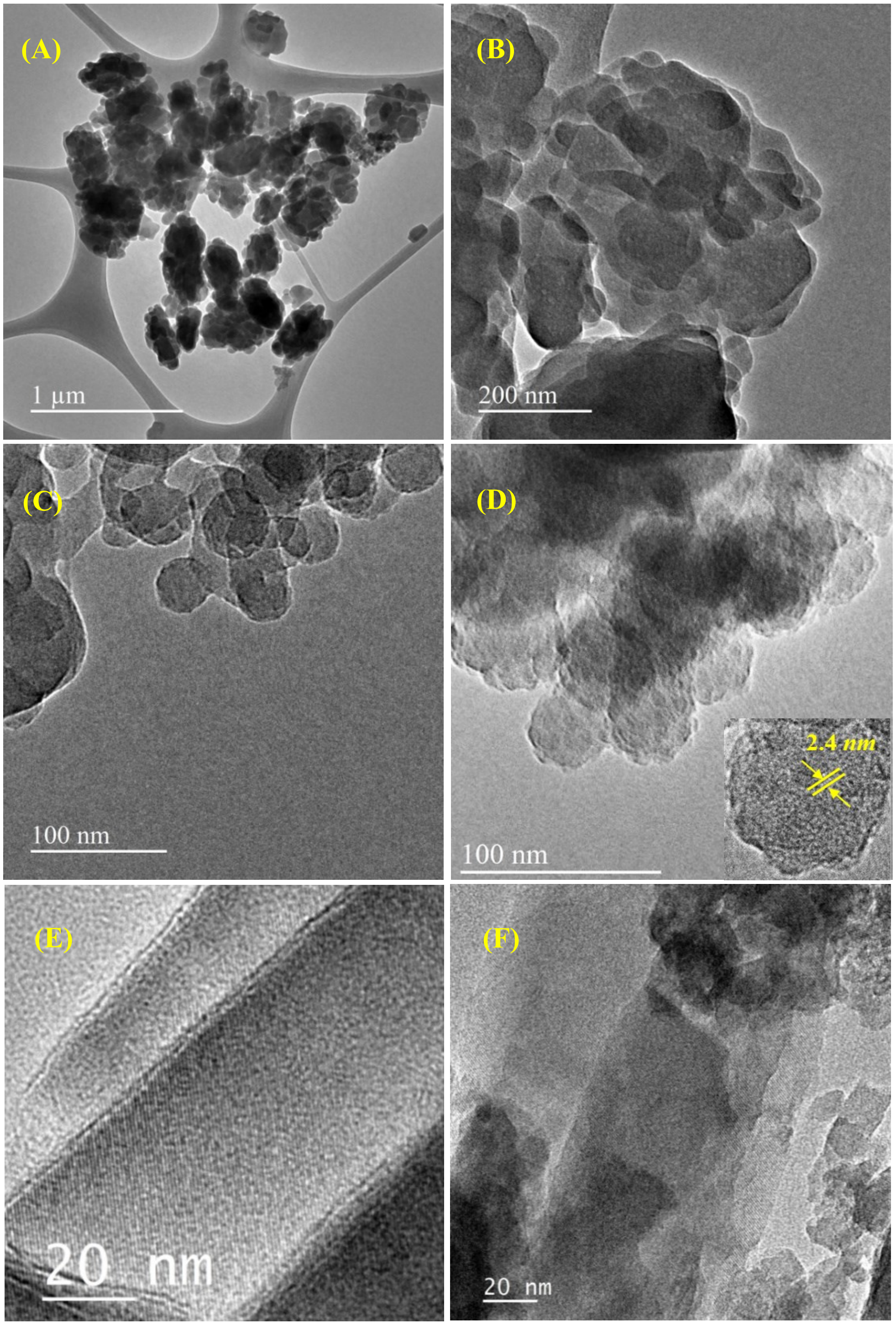

Figure S6. TEM images of *n*-ZSM-5 (A-D) and ZSM-5 (E,F).

Deconvoluted Infrared Spectra

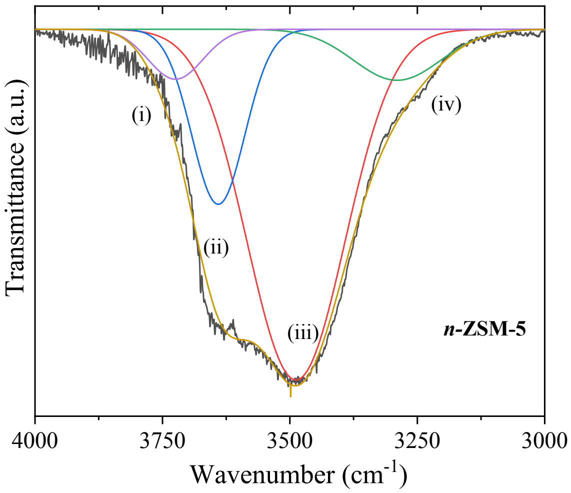
Transmittance (a.u.)
(i)
(ii)
(iii)
(iv)
n-ZSM-5
4000
3750
3500
3250
3000
Wavenumber (cm-1)

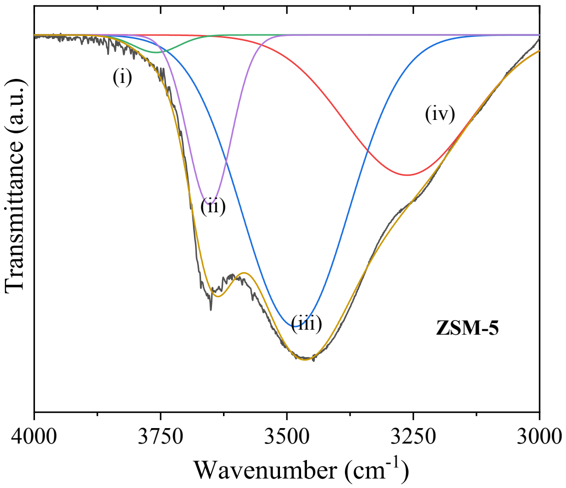
Transmittance (a.u.)
(i)
(ii)
(iii)
(iv)
ZSM-5
4000
3750
3500
3250
3000
Wavenumber (cm-1)

Figure S7. Deconvoluted Infrared spectra of nano- and bulk ZSM-5 based on the hydroxyl stretching frequency: (i) isolated silanol (3745 cm^{-1}); (ii) bridging silanol (3646 cm^{-1}); (iii) silanol nest (3646 cm^{-1}); (iv) adsorbed water (3247 cm^{-1}).

References

[1] P. Selvam, N. V. Krishna and A. Sakthivel, Adv. Porous Mater. **1**, 239 (2013).

[2] G. Kresse and J. Hafner, Phys. Rev. B **47**, 558 (1993); **49**, 14251 (1994).

[3] G. Kresse and J. Furthmüller, Phys. Rev. B **54**, 11169 (1996); Comput. Mater. Sci. **6**, 15 (1996).

[4] J.P. Perdew, K. Burke and M. Ernzerhof, Phys. Rev. Lett. **77**, 3865 (1996).

[5] W. Kohn and L.J. Sham, Phys. Rev. **140**, A1133 (1965).

[6] P.E. Blöchl, Phys. Rev. B **50**, 17953 (1994).

[7] G. Kresse and D. Joubert, Phys. Rev. B **59**, 1758 (1999).

[8] H. Monkhorst and J. Pack, Phys. Rev. B **13**, 5188 (1976).

[9] K.M. Ho, C.L. Fu, B.N. Harmon, W. Weber and D.R. Hamann, Phys. Rev. Lett. **49**, 673 (1982).

[10] C.L. Fu and K.M. Ho, Phys. Rev. B **28**, 5480 (1983).

[11] M. Methfessel and A.T. Paxton, Phys. Rev. B **40**, 3616 (1989).

[12] S. Grimme, J. Antony, S. Ehrlich and H. Krieg, J. Chem. Phys. **132**, 154104 (2010).

[13] S. Grimme, S. Ehrlich and L. Goerigk, J. Comput. Chem. **32**, 1456 (2011).

[14] R.B. McClurg, J. Chem. Phys. **117**, 5328 (2002).

[15] M. Carpineti, F. Ferri, M. Giglio, E. Paganini, and U. Perini, Phys. Rev. A **42**, 7347 (1990).